

Observation of the Decay $B^0 \rightarrow J/\psi\eta$

M.-C. Chang,⁵ K. Abe,⁸ K. Abe,⁴³ I. Adachi,⁸ H. Aihara,⁴⁵ D. Anipko,¹ K. Arinstein,¹ T. Aushev,^{18,13} A. M. Bakich,⁴⁰ E. Barberio,²⁰ A. Bay,¹⁸ I. Bedny,¹ K. Belous,¹² U. Bitenc,¹⁴ I. Bizjak,¹⁴ S. Blyth,²³ A. Bondar,¹ A. Bozek,²⁶ T. E. Browder,⁷ P. Chang,²⁵ Y. Chao,²⁵ A. Chen,²³ K.-F. Chen,²⁵ W. T. Chen,²³ B. G. Cheon,³ R. Chistov,¹³ S.-K. Choi,⁵¹ Y. Choi,³⁹ Y. K. Choi,³⁹ S. Cole,⁴⁰ J. Dalseno,²⁰ M. Danilov,¹³ M. Dash,⁴⁹ A. Drutskoy,⁴ S. Eidelman,¹ S. Fratina,¹⁴ N. Gabyshev,¹ T. Gershon,⁸ A. Go,²³ G. Gokhroo,⁴¹ H. Ha,¹⁶ J. Haba,⁸ T. Hara,³¹ K. Hayasaka,²¹ M. Hazumi,⁸ D. Heffernan,³¹ T. Hokuue,²¹ Y. Hoshi,⁴³ S. Hou,²³ W.-S. Hou,²⁵ Y. B. Hsiung,²⁵ T. Iijima,²¹ K. Inami,²¹ A. Ishikawa,⁴⁵ H. Ishino,⁴⁶ R. Itoh,⁸ M. Iwasaki,⁴⁵ Y. Iwasaki,⁸ H. Kaji,²¹ J. H. Kang,⁵⁰ S. U. Kataoka,²² H. Kawai,² T. Kawasaki,²⁸ H. R. Khan,⁴⁶ H. Kichimi,⁸ S. K. Kim,³⁷ Y. J. Kim,⁶ K. Kinoshita,⁴ S. Korpar,^{19,14} P. Križan,^{52,14} P. Krokovny,⁸ R. Kulasiri,⁴ R. Kumar,³² C. C. Kuo,²³ A. Kuzmin,¹ Y.-J. Kwon,⁵⁰ G. Leder,¹¹ M. J. Lee,³⁷ S. E. Lee,³⁷ T. Lesiak,²⁶ A. Limosani,⁸ S.-W. Lin,²⁵ G. Majumder,⁴¹ F. Mandl,¹¹ T. Matsumoto,⁴⁷ A. Matyja,²⁶ S. McOnie,⁴⁰ W. Mitaroff,¹¹ K. Miyabayashi,²² H. Miyake,³¹ H. Miyata,²⁸ Y. Miyazaki,²¹ R. Mizuk,¹³ T. Mori,²¹ T. Nagamine,⁴⁴ I. Nakamura,⁸ E. Nakano,³⁰ M. Nakao,⁸ S. Nishida,⁸ O. Nitoh,⁴⁸ S. Noguchi,²² S. Ogawa,⁴² T. Ohshima,²¹ S. Okuno,¹⁵ S. L. Olsen,⁷ Y. Onuki,³⁴ H. Ozaki,⁸ P. Pakhlov,¹³ G. Pakhlova,¹³ H. Palka,²⁶ H. Park,¹⁷ K. S. Park,³⁹ L. S. Peak,⁴⁰ R. Pestotnik,¹⁴ L. E. Piilonen,⁴⁹ Y. Sakai,⁸ N. Satoyama,³⁸ T. Schietinger,¹⁸ O. Schneider,¹⁸ J. Schümann,²⁴ A. J. Schwartz,⁴ R. Seidl,^{9,34} K. Senyo,²¹ M. Shapkin,¹² H. Shibuya,⁴² B. Shwartz,¹ J. B. Singh,³² A. Somov,⁴ N. Soni,³² S. Stanič,²⁹ M. Starič,¹⁴ H. Stoeck,⁴⁰ K. Sumisawa,⁸ T. Sumiyoshi,⁴⁷ S. Suzuki,³⁵ O. Tajima,⁸ F. Takasaki,⁸ K. Tamai,⁸ N. Tamura,²⁸ M. Tanaka,⁸ G. N. Taylor,²⁰ Y. Teramoto,³⁰ X. C. Tian,³³ I. Tikhomirov,¹³ K. Trabelsi,⁷ T. Tsuboyama,⁸ T. Tsukamoto,⁸ S. Uehara,⁸ T. Uglov,¹³ S. Uno,⁸ P. Urquijo,²⁰ Y. Ushiroda,⁸ Y. Usov,¹ G. Varner,⁷ K. E. Varvell,⁴⁰ S. Villa,¹⁸ C. C. Wang,²⁵ C. H. Wang,²⁴ M.-Z. Wang,²⁵ Y. Watanabe,⁴⁶ R. Wedd,²⁰ E. Won,¹⁶ Q. L. Xie,¹⁰ A. Yamaguchi,⁴⁴ Y. Yamashita,²⁷ M. Yamauchi,⁸ Y. Yusa,⁴⁹ C. C. Zhang,¹⁰ L. M. Zhang,³⁶ Z. P. Zhang,³⁶ and A. Zupanc¹⁴

(Belle Collaboration)

¹*Budker Institute of Nuclear Physics, Novosibirsk*²*Chiba University, Chiba*³*Chonnam National University, Kwangju*⁴*University of Cincinnati, Cincinnati, Ohio 45221*⁵*Department of Physics, Fu Jen Catholic University, Taipei*⁶*The Graduate University for Advanced Studies, Hayama*⁷*University of Hawaii, Honolulu, Hawaii 96822*⁸*High Energy Accelerator Research Organization (KEK), Tsukuba*⁹*University of Illinois at Urbana-Champaign, Urbana, Illinois 61801*¹⁰*Institute of High Energy Physics, Chinese Academy of Sciences, Beijing*¹¹*Institute of High Energy Physics, Vienna*¹²*Institute of High Energy Physics, Protvino*¹³*Institute for Theoretical and Experimental Physics, Moscow*¹⁴*J. Stefan Institute, Ljubljana*¹⁵*Kanagawa University, Yokohama*¹⁶*Korea University, Seoul*¹⁷*Kyungpook National University, Taegu*¹⁸*Swiss Federal Institute of Technology of Lausanne, EPFL, Lausanne*¹⁹*University of Maribor, Maribor*²⁰*University of Melbourne, Victoria*²¹*Nagoya University, Nagoya*²²*Nara Women's University, Nara*²³*National Central University, Chung-li*²⁴*National United University, Miao Li*²⁵*Department of Physics, National Taiwan University, Taipei*²⁶*H. Niewodniczanski Institute of Nuclear Physics, Krakow*²⁷*Nippon Dental University, Niigata*²⁸*Niigata University, Niigata*²⁹*University of Nova Gorica, Nova Gorica*³⁰*Osaka City University, Osaka*

- ³¹Osaka University, Osaka
³²Panjab University, Chandigarh
³³Peking University, Beijing
³⁴RIKEN BNL Research Center, Upton, New York 11973
³⁵Saga University, Saga
³⁶University of Science and Technology of China, Hefei
³⁷Seoul National University, Seoul
³⁸Shinshu University, Nagano
³⁹Sungkyunkwan University, Suwon
⁴⁰University of Sydney, Sydney NSW
⁴¹Tata Institute of Fundamental Research, Bombay
⁴²Toho University, Funabashi
⁴³Tohoku Gakuin University, Tagajo
⁴⁴Tohoku University, Sendai
⁴⁵Department of Physics, University of Tokyo, Tokyo
⁴⁶Tokyo Institute of Technology, Tokyo
⁴⁷Tokyo Metropolitan University, Tokyo
⁴⁸Tokyo University of Agriculture and Technology, Tokyo
⁴⁹Virginia Polytechnic Institute and State University, Blacksburg, Virginia 24061
⁵⁰Yonsei University, Seoul
⁵¹Gyeongsang National University, Chinju
⁵²University of Ljubljana, Ljubljana
(Received 1 January 2007; published 30 March 2007)

We report the first observation of $B^0 \rightarrow J/\psi \eta$ decay. These results are obtained from a data sample that contains 449×10^6 $B\bar{B}$ pairs accumulated at the $Y(4S)$ resonance with the Belle detector at the KEKB asymmetric-energy e^+e^- collider. We observe a signal with a significance of 8.1σ and obtain a branching fraction of $(9.5 \pm 1.7(\text{stat}) \pm 0.8(\text{syst})) \times 10^{-6}$.

DOI: 10.1103/PhysRevLett.98.131803

PACS numbers: 13.25.Hw, 14.40.Aq, 14.40.Nd

At the quark level, the decay $B^0 \rightarrow J/\psi \eta$ proceeds primarily via a $\bar{b} \rightarrow \bar{c} d \bar{d}$ transition. As is apparent from its Feynman diagram (Fig. 1), this is a Cabibbo- and color-suppressed decay, similar to $B^0 \rightarrow J/\psi \pi^0$ for which the branching fraction and CP violation parameters have been measured by the BABAR and Belle Collaborations [1–6]. The best existing limit for the branching fraction for $B^0 \rightarrow J/\psi \eta$ comes from BABAR [7] and is based on 56×10^6 $B\bar{B}$ pairs.

If factorization and flavor-SU(3) symmetric coefficients for the $\bar{d}d$ content are assumed, the branching fraction for $B^0 \rightarrow J/\psi \eta$ decay is expected to be comparable to that for $B^0 \rightarrow J/\psi \pi^0$. If the measured branching fraction is significantly different from this expectation, it would imply the influence of large final-state interactions or nonstandard contributions. In the latter case, precise measurements of CP violation parameters might also reveal unexpected phenomena.

In this Letter, we report the first observation of the decay $B^0 \rightarrow J/\psi \eta$ [8]. The measurement is based on a data sample that contains 449×10^6 $B\bar{B}$ pairs, collected with the Belle detector at the KEKB asymmetric-energy e^+e^- (3.5 on 8 GeV) collider [9] operating at the $Y(4S)$ resonance.

The Belle detector is a large-solid-angle magnetic spectrometer that consists of a silicon vertex detector (SVD), a 50-layer central drift chamber (CDC), an array of aerogel

threshold Čerenkov counters (ACC), a barrel-like arrangement of time-of-flight (TOF) scintillation counters, and an electromagnetic calorimeter comprised of CsI(Tl) crystals (ECL). All these detectors are located inside a superconducting solenoid coil that provides a 1.5 T magnetic field. An iron flux-return located outside of the coil is instrumented to detect K_L^0 mesons and to identify muons (KLM). The detector is described in detail elsewhere [10].

The data used in this analysis were collected with two detector configurations. A 2.0 cm radius beam pipe and a 3-layer silicon vertex detector are used for the first sample of 152×10^6 $B\bar{B}$ pairs, while a 1.5 cm radius beam pipe, a 4-layer silicon detector, and a small-cell inner drift chamber are used to record the remaining 297×10^6 $B\bar{B}$ pairs [11]. A GEANT-based Monte Carlo (MC) simulation is used to model the response of the detector and determine efficiencies [12].

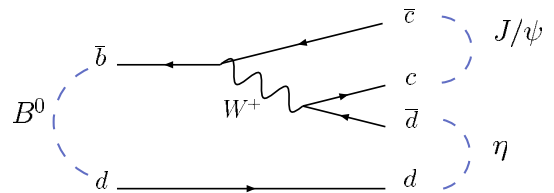


FIG. 1 (color online). Feynman diagram for the leading contribution to the decay $B^0 \rightarrow J/\psi \eta$.

Charged tracks are selected based on the impact parameters relative to the interaction point: dr for the radial direction and dz for the direction along the positron beam. Our requirements are $dr < 1$ cm and $|dz| < 5$ cm. From among the selected charged tracks, e^+ and e^- candidates are identified by combining information from the ECL, the CDC (dE/dx), and the ACC. Identification of μ^+ and μ^- candidates is based on track penetration depth and the hit pattern in the KLM system. Charged pions are identified using the combined information from the CDC (dE/dx), the TOF, and the ACC.

Photon candidates are selected from calorimeter showers not associated with charged tracks. An energy deposition with a photonlike shape and with energy of at least 50 MeV in the barrel region or 100 MeV in the end cap region is considered a photon candidate. A pair of photons with an invariant mass $117.8 \text{ MeV}/c^2 < M_{\gamma\gamma} < 150.2 \text{ MeV}/c^2$ is considered as a π^0 candidate. This invariant mass region corresponds to a $\pm 3\sigma$ interval around the π^0 mass, where σ is the mass resolution.

We reconstruct J/ψ mesons in the $\ell^+\ell^-$ decay channel ($\ell = e$ or μ) and include up to one bremsstrahlung photon that is within 50 mrad of each of the e^+ and e^- tracks (denoted as $e^+e^-(\gamma)$). The invariant mass is required to be within $-0.15 \text{ GeV}/c^2 < M_{ee(\gamma)} - m_{J/\psi} < 0.036 \text{ GeV}/c^2$ and $-0.06 \text{ GeV}/c^2 < M_{\mu\mu} - m_{J/\psi} < 0.036 \text{ GeV}/c^2$, where $m_{J/\psi}$ denotes the nominal mass, $M_{ee(\gamma)}$ and $M_{\mu\mu}$ are the reconstructed invariant mass from $e^+e^-(\gamma)$ and $\mu^+\mu^-$, respectively. Asymmetric intervals are used to include part of the radiative tails.

Candidate η mesons are reconstructed in the $\gamma\gamma$ and $\pi^+\pi^-\pi^0$ final states. We require the invariant mass to be in the range $500 \text{ MeV}/c^2 < M_{\gamma\gamma} < 575 \text{ MeV}/c^2 (\pm 3\sigma)$ and $535 \text{ MeV}/c^2 < M_{\pi^+\pi^-\pi^0} < 560 \text{ MeV}/c^2 (\pm 3\sigma)$. In the $\gamma\gamma$ final state, we remove η candidates if either of the daughter photons form a π^0 candidate when combined with any other photon in the event. Asymmetric decays are removed with the requirement $|E_{\gamma 1} - E_{\gamma 2}|/(E_{\gamma 1} + E_{\gamma 2}) < 0.8$, where $E_{\gamma 1}$ and $E_{\gamma 2}$ are the energies of the two photons that form the η candidate.

We combine the J/ψ and η to form B mesons. Signal candidates are identified by two kinematic variables defined in the $Y(4S)$ center-of-mass (c.m.) frame: the beam-energy constrained mass, $M_{bc} = \sqrt{E_{\text{beam}}^2 - p_B^{*2}}$, and the energy difference, $\Delta E = E_B^* - E_{\text{beam}}$, where p_B^* and E_B^* are the momentum and energy of the B candidate and E_{beam} is the run-dependent beam energy. To improve the ΔE resolution, the masses of the selected π^0 , η , and J/ψ candidates are constrained to their nominal masses using mass-constrained kinematic fits. In addition, vertex-constrained fits are applied to the $\eta \rightarrow \pi^+\pi^-\pi^0$ and $J/\psi \rightarrow \ell^+\ell^-$ candidates. We retain events with $M_{bc} > 5.2 \text{ GeV}/c^2$ and $|\Delta E| < 0.2 \text{ GeV}$, and define a signal region to be $5.27 \text{ GeV}/c^2 < M_{bc} < 5.29 \text{ GeV}/c^2$,

$-0.10 \text{ GeV} < \Delta E < 0.05 \text{ GeV}$ ($\eta \rightarrow \gamma\gamma$), or $|\Delta E| < 0.05 \text{ GeV}$ ($\eta \rightarrow \pi^+\pi^-\pi^0$). In events with more than one B candidate, usually due to multiple η candidates, the B candidate with the minimum χ^2 value from the mass- and vertex-constrained fit is chosen.

To suppress the combinatorial background dominated by the two-jet-like $e^+e^- \rightarrow q\bar{q}$ ($q = u, d, s$) continuum process, we remove events with the ratio of second to zeroth Fox-Wolfram moments $R_2 > 0.4$ [13]. This requirement is determined using a figure-of-merit $N_S/\sqrt{N_S + N_B}$, where N_S is the number of expected signal events and N_B is the number of background events. For N_S , we use a MC simulation with the assumption that $\mathcal{B}(B^0 \rightarrow J/\psi\eta)$ is 6×10^{-6} [14]. For N_B , we use a sample of continuum background MC data that corresponds to an integrated luminosity that is about 3 times that of the data sample and normalized to the number of events in an $M_{bc} - \Delta E$ sideband ($5.2 \text{ GeV}/c^2 < M_{bc} < 5.26 \text{ GeV}/c^2$ and $0.1 \text{ GeV} < \Delta E < 0.2 \text{ GeV}$). This requirement on R_2 eliminates 88% of the continuum background and retains 97% of the signal.

After the above continuum suppression, the background is dominated by $B\bar{B}$ events with B decays to J/ψ . We use a MC sample corresponding to 3.86×10^{10} generic $B\bar{B}$ decays that includes all known $B^0 \rightarrow J/\psi X$ processes to investigate these backgrounds. We find that the dominant backgrounds come from $B^0 \rightarrow J/\psi K_L$ (25.1%), $B^\pm \rightarrow J/\psi K^{*\pm}$ (892) (19.3%), $B^0 \rightarrow J/\psi K^{*0}$ (892) (14.5%), $B^0 \rightarrow J/\psi K_S$ (14.1%), $B^0 \rightarrow J/\psi \pi^0$ (8.4%), and a few other exclusive $B \rightarrow J/\psi X$ decay modes. These backgrounds peak in the M_{bc} distributions but not in ΔE . Thus, the shape of the ΔE distribution for combinatorial backgrounds from $B \rightarrow J/\psi X$ decays is distinct from that of the signal and does not affect the signal yield extracted from that distribution.

Signal yields and background levels are determined by fitting the distributions in ΔE for candidates in the M_{bc} signal region. The ΔE distribution is fitted with a function that is the sum of a crystal ball line function [15] and two Gaussians for signal, and a second-order polynomial for background. The probability density functions (PDF) that describe the signal and background shapes are determined from MC simulations. We use the MC sample for this process to determine the PDF for the total background.

We use the decay $B^+ \rightarrow J/\psi K^{*+}$ ($K^{*+} \rightarrow K^+\pi^0$) as a control sample to correct for differences between data and MC calculations for the fitted mean and width values of the ΔE signal peak. For this selection, we require the helicity angle in the $K^{*+} \rightarrow K^+\pi^0$ decay, i.e., the angle between the π^0 and the negative of the B^+ momenta in the K^* rest frame, to be less than 86° . This requirement primarily selects events with a high momentum π^0 and produces a control-sample ΔE distribution that is similar to that for our signal decay mode. The signal PDF is modified based on the results for the control sample: the mean value of ΔE

is shifted by -3.81 ± 0.65 MeV and the width is scaled by a factor of 0.99 ± 0.04 .

There are 98 and 58 events in the $M_{B\bar{B}}$ signal region for the $\eta \rightarrow \gamma\gamma$ and $\eta \rightarrow \pi^+\pi^-\pi^0$ modes, respectively. We determine the signal content by performing an unbinned extended maximum-likelihood fit to the candidate data events. The unbinned extended maximum-likelihood function is

$$\mathcal{L} = \frac{e^{-(N_S+N_B)}}{N!} \prod_i [N_S P_S(\Delta E_i) + N_B P_B(\Delta E_i)], \quad (1)$$

where N is the total number of candidate events, N_S and N_B denote the number of signal and $B\bar{B}$ background events, $P_S(\Delta E_i)$ and $P_B(\Delta E_i)$ denote the signal and background ΔE PDFs, respectively, and i is the event index. Separate fits to the $B^0 \rightarrow J/\psi\eta(\gamma\gamma)$ and $B^0 \rightarrow J/\psi\eta(\pi^+\pi^-\pi^0)$ candidate samples give signal yields of 43.1 ± 8.9 and 16.6 ± 5.8 events, respectively. The results of the fits to the data are shown in Fig. 2. These signal yields correspond to branching fractions of $(9.6 \pm 1.9) \times 10^{-6}$ and $(10.0 \pm 3.5) \times 10^{-6}$, respectively. We fit the two samples simultaneously, constraining the results to a common branching fraction, and obtain 59.7 ± 10.5 events. The combined branching fraction is $(9.5 \pm 1.7) \times 10^{-6}$.

We correct for discrepancies of the signal detection efficiency between data and MC calculations using control samples. The $J/\psi \rightarrow \mu^+\mu^-$ and $D^{*+} \rightarrow D^0\pi^+$ ($D^0 \rightarrow K^-\pi^+$) events are used as control samples to correct for the muon identification and pion identification, respectively. We find that the MC simulation overestimates the efficiencies for $J/\psi \rightarrow \mu^+\mu^-$ and $\eta \rightarrow \pi^+\pi^-\pi^0$ by 8.5% and 1.8%, respectively.

A 4.8% systematic error associated with uncertainties in the signal and background PDFs is estimated by comparing the fit results for the cases when the polynomial parameters are fixed by either MC or data in the $M_{B\bar{B}}$ sideband region, and from changes that result from varying each parameter by 1 standard deviation. For the contribution from the

corrections to the lepton identification efficiencies, we use a control sample of $J/\psi \rightarrow \ell^+\ell^-$, which indicates uncertainties of 2.7% per electron track and 1.2% per muon track. By weighting the relative contributions from $J/\psi \rightarrow e^+e^-$ and $J/\psi \rightarrow \mu^+\mu^-$, we assign a 3.9% systematic error. The systematic error from the pion identification correction is 0.7% per track; this is determined from a study of the $D^{*+} \rightarrow D^0\pi^+$ ($D^0 \rightarrow K^-\pi^+$) control sample. Since this applies only to the $\eta \rightarrow \pi^+\pi^-\pi^0$ decay mode, the effective systematic error is 0.4%. The systematic error due to the track finding efficiencies for the Belle detector is 1.0% per charged lepton and 1.3% per charged pion. This contributes 2% per J/ψ and 0.7% per η , and the total of 2.7% (from linearly adding) is included. A 4.1% systematic error due to π^0 detection is determined from a comparison of the data and MC ratios for a large sample of $\eta \rightarrow \pi^+\pi^-\pi^0$ and $\eta \rightarrow 3\pi^0$ decays. Since $\eta \rightarrow \gamma\gamma$ is similar to π^0 decay, we also assign 4.1% as the systematic error for $\eta \rightarrow \gamma\gamma$ reconstruction. The errors on the branching fractions for $J/\psi \rightarrow \ell^+\ell^-$, $\eta \rightarrow \gamma\gamma$, and $\eta \rightarrow \pi^+\pi^-\pi^0$ are 1.0%, 0.7%, and 1.8%, respectively [16]. These errors contribute 1% and 1.1% systematic errors due to $\mathcal{B}(J/\psi \rightarrow \ell^+\ell^-)$ and $\mathcal{B}(\eta \rightarrow \gamma\gamma \text{ and } \pi^+\pi^-\pi^0)$, respectively. We assign a systematic error of 1.2% due to the uncertainty in the number of $B\bar{B}$ pairs.

The systematic errors are summarized in Table I. The total uncertainty is the quadratic sum of each term. The detection efficiencies and branching fractions are listed in Table II. The statistical significance of the observed signal, defined as $\sqrt{-2\ln(\mathcal{L}_0/\mathcal{L}_{\max})}$, where \mathcal{L}_{\max} (\mathcal{L}_0) denotes the likelihood value at the maximum (with the signal yield fixed at zero), is 8.1σ .

In summary, the first observation of the decay $B^0 \rightarrow J/\psi\eta$ is reported. We observe 59.7 ± 10.5 signal events with 8.1σ significance in a $449 \times 10^6 B\bar{B}$ pair data sample at the $Y(4S)$ resonance. The measured branching fraction is $\mathcal{B}(B^0 \rightarrow J/\psi\eta) = (9.5 \pm 1.7 \pm 0.8) \times 10^{-6}$, where the first error is statistical and the second is systematic. The measured branching fraction is consistent with theoretical expectations based on the measured $J/\psi\pi^0$ branching

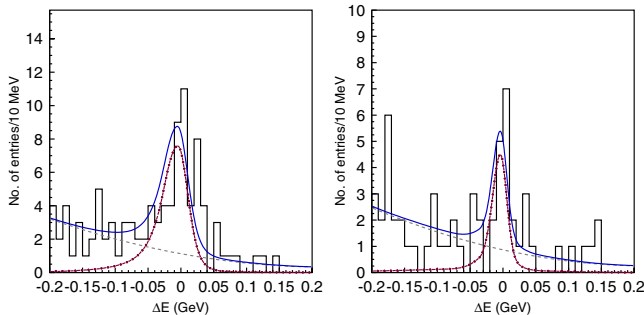


FIG. 2 (color online). ΔE distributions for the decay $B^0 \rightarrow J/\psi\eta$. The plot on the left shows $B^0 \rightarrow J/\psi\eta(\eta \rightarrow \gamma\gamma)$, while $B^0 \rightarrow J/\psi\eta(\eta \rightarrow \pi^+\pi^-\pi^0)$ is on the right. The curves show the signal (dash-dot lines) and background (dashed lines) contributions as well as the overall fit (solid lines).

TABLE I. Systematic errors for the combined branching fraction.

	Systematic errors (%)
PDFs	4.8
Lepton identification	3.9
Charged pion identification	0.4
Tracking (lepton and charged pion)	2.7
$\eta \rightarrow \gamma\gamma$, π^0 selection	4.1
$\mathcal{B}(J/\psi \rightarrow \ell^+\ell^-)$	1.0
$\mathcal{B}(\eta \rightarrow \gamma\gamma \text{ and } \pi^+\pi^-\pi^0)$	1.1
$N_{B\bar{B}}$	1.2
Total	8.1

TABLE II. Detection efficiencies and branching fractions (BF).

Mode	Eff.(%)	BF(10^{-6})
$B^0 \rightarrow J/\psi\eta(\gamma\gamma)$	21.9	9.6 ± 1.9
$B^0 \rightarrow J/\psi\eta(\pi^+\pi^-\pi^0)1$	13.8	10.0 ± 3.5
$B^0 \rightarrow J/\psi\eta$ (combined)		$9.5 \pm 1.7 \pm 0.8$

fraction [16,17]. There is no indication of either large final-state interactions or nonstandard model contributions.

We thank the KEKB group for excellent operation of the accelerator, the KEK cryogenics group for efficient solenoid operations, and the KEK computer group and the NII for valuable computing and Super-SINET network support. We acknowledge support from MEXT and JSPS (Japan); ARC and DEST (Australia); NSFC and KIP of CAS (Contract No. 10575109 and IHEP-U-503, China); DST (India); the BK21 program of MOEHRD, and the CHEP SRC and BR (Grant No. R01-2005-000-10089-0) programs of KOSEF (Korea); KBN (Contract No. 2P03B 01324, Poland); MIST (Russia); ARRS (Slovenia); SNSF (Switzerland); NSC and MOE (Taiwan); and DOE (USA).

[1] P. Avery *et al.* (CLEO Collaboration), Phys. Rev. D **62**, 051101 (2000).

[2] B. Aubert *et al.* (BABAR Collaboration), Phys. Rev. D **65**, 032001 (2002).
[3] K. Abe *et al.* (Belle Collaboration), Phys. Rev. D **67**, 032003 (2003).
[4] B. Aubert *et al.* (BABAR Collaboration), Phys. Rev. Lett. **91**, 061802 (2003).
[5] S. U. Kataoka *et al.* (Belle Collaboration), Phys. Rev. Lett. **93**, 261801 (2004).
[6] B. Aubert *et al.* (BABAR Collaboration), Phys. Rev. D **74**, 011101 (2006).
[7] B. Aubert *et al.* (BABAR Collaboration), Phys. Rev. Lett. **91**, 071801 (2003).
[8] Inclusion of charge conjugate modes is implied.
[9] S. Kurokawa and E. Kikutani, Nucl. Instrum. Methods Phys. Res., Sect. A **499**, 1 (2003), and other papers included in this volume.
[10] A. Abashian *et al.* (Belle Collaboration), Nucl. Instrum. Methods Phys. Res., Sect. A **479**, 117 (2002).
[11] Z. Natkaniec (Belle SVD2 Group), Nucl. Instrum. Methods Phys. Res., Sect. A **560**, 1 (2006).
[12] R. Brun *et al.*, GEANT 3.21, CERN Report No. DD/EE/84-1, 1984.
[13] The Fox-Wolfram moments were introduced in G. C. Fox and S. Wolfram, Phys. Rev. Lett. **41**, 1581 (1978).
[14] For this optimization, we assume a branching fraction for $J/\psi\eta$ that is about one third that for $J/\psi\pi^0$.
[15] DESY Internal Report, DESY Report No. F31-86-02 1990.
[16] W.-M. Yao *et al.* (Particle Data Group), J. Phys. G **33**, 1 (2006).
[17] A. Deandrea *et al.*, Phys. Lett. B **318**, 549 (1993).